Bioresource Technology Reports 34 (2026) 102671

Contents lists available at ScienceDirect

Bioresource Technology Reports

journal homepage: www.sciencedirect.com/journal/bioresource-technology-reports

Integrated electro-oxidation using a hollow cylindrical Ti–TiO_2/IrO_2/RuO_2 mesh electrode and biodegradation for sustainable treatment of hospital wastewater

Vinoth Kumar Palur Manoharan [a], Madhan Kumar Pichandi [b], Adikesavan Selvi [c], Babujanarthanam Ranganathan [b], Sudharsan Kasirajan [a,*]

[a] Department of Microbiology, Vels Institute of Science and Technology & Advanced Studies (VISTAS) pallavaram, Chennai, Tamil Nadu, 600117, India
[b] Nano & Energy Bio Science Laboratory, Department of Biotechnology, Thiruvalluvar University, Serkkadu, Vellore, Tamilnadu, 632115, India
[c] Central Research Facility, Dr. MGR Educational and Research Institute, Dr. MGR University, Chennai, Tamilnadu, 600095, India

ARTICLE INFO

Keywords:
Hospital wastewater
Electro-oxidation
Biodegradation
Priestia flexa
Phytotoxicity
Ecotoxicology

ABSTRACT

Raw hospital wastewater has high organic load, active pharmaceutical residues and alarming environmental parameters, thus posing a significant environmental risk. This study assesses the electro-oxidation (EO) of hospital wastewater (HWW) using a Ti–TiO_2/IrO_2/RuO_2 mesh electrode under optimal conditions, and the demineralised intermediate organic compounds are degraded through microbial processes. 16S rRNA phylogenetics confirmed the isolated bacterium as *Priestia flexa,* which played a major role in biodegradation. At the end of 20d, significant reductions of 96% decrease in COD, a 95% reduction in BOD, and an 85% decline in TOC. HR-SEM and EDAX analysis suggested a robost and consistent electrode design and performance throughout several EO cycles. FTIR and GC–MS studies revealed elimination of key functional groups. In addition, Ecotoxicological evaluations of water quality and Phytotoxicity studies demonstrated positive outcomes with an integrated approach treated HWW. Embryonic toxicity in Zebra fish with treated wastewater resulted in normal embryonic development up to 72 hpf, even at 25 µL. Hence, the integrated approach has found to be efficient in treating HWW.

1. Introduction

Hospital wastewater (HWW) is an emerging class of complex and potentially hazardous effluent of concern in the global scenario as it contains complex, multidrug resistance characteristics, diverse conglomerate of hazardous effluent and repository of antimicrobial resistance (Kumari et al., 2020). Pharmaceutical residues, cytotoxic drugs, disinfectants, solvents, pathogenic microorganisms, antibiotic-resistant microbes, heavy metals, radioactive isotopes, along with metabolic by-products of therapeutic interventions are just a few of the unique contaminants found in industrial and hospital effluents, which come from a variety of medical, surgical, diagnostic, and research activities (Pariente et al., 2022). They contribute to create a toxic mixture that poses a threat not only to aquatic ecosystems but also to agricultural systems, to public health, and threat to long-term biodiversity (Ogwu et al., 2025). Untreated or inadequately treated HWW is directly discharged into sewers thus the receiving water bodies have a contributory role in soil/groundwater contamination, eutrophication, bioaccumulation, endocrine disruption, teratogenic effects, and dissemination of resistant strains of microbial agents (Oliveira, 2018).

Conventional hospital wastewater is characterized by high physicochemical loads includes high Chemical Oxygen demand (COD), biochemical Oxygen demand (BOD), Total dissolved solids (TDS), Total suspended solids (TSS), and chloride concentrations, with its dark brown coloration, foul odour evocative of rotten eggs (hydrogen sulphide, H_2S), ammonia (NH_3) and presence of volatile organic hydrocarbons making it olfactory distinct from other forms of wastewater (Akin, 2016; Devda et al., 2021). Though numerous methods of remediation have been reported so far Electro- oxidation (EO) is one effective method based on the principle of anodic oxidation in which pollutants are directly oxidized on the electrode surface or indirectly oxidized through the electrochemical generation of species like hydroxyl radicals (•OH), hydrogen peroxide, ozone, and active chlorine (HOCl, OCl^-), and electrodes, including dimensionally stable anodes (DSAs) such as Titanium

* Corresponding author.
E-mail address: ksudharsan.sls@vistas.ac.in (S. Kasirajan).

https://doi.org/10.1016/j.biteb.2026.102671
Received 3 November 2025; Received in revised form 23 February 2026; Accepted 26 February 2026
Available online 5 March 2026

(Ti)–Titanium Dioxide (TiO_2) / Iridium Oxide (IrO_2) / Ruthenium Oxide (RuO_2). These electrodes are most widely adopted for their chemical stability, conductivity, and high oxidation capacity, thus allowing rapid COD and BOD removal, pathogenic inactivation, and partial mineralization of complex individuals, as reported in earlier studies (Bhandari et al., 2023; Vinoth et al., 2025). Hence, the choice and design of the electrode makes EO process much more effective. In this regard, we have designed a hollow cylindrical pattern mesh electrode and have explored for the present study.

Integrated processes are the combination of two different methods that are gaining high popularity as it is reported to achieve effective remediation in various environmental matrices and will address a major drawback of large-scale implementation (Selvi et al., 2019). Herein, we report on one of the integrated process of EO and microbial mediated biodegradation that would prove as a sustainable hybrid strategy, where EO serves as a pretreatment to reduce the high-bulk contaminant concentration, eliminate pathogens, and convert recalcitrant organics to more biodegradable intermediates that can be further efficiently mineralized by microbial communities as evidenced in previous studies (Oluwole et al., 2020; Nidheesh et al., 2022).

Priestia flexa is a gram-positive, rod-shaped, spore-forming, halo tolerant bacterium isolated from HWW with 16S rRNA sequence similarity (99.7%, GenBank accession PQ220112) that exhibits excellent potential of biodegradation in HWW. Though EO follows radical-driven pathways wherein hydroxyl radical and active chlorine species attack bonds non-selective leading to oxidative cleavage of non-activated bonds and rapid decolorization. Biodegradation follows substrate-specific enzymatic pathways that are slower but aids in complete and environmentally friendly mineralization of the toxic compounds (Bagade and Doke, 2025).

This combined EO-biodegradation process was highly efficient in not only removing chemical pollutants, but also ensured environmental security, which was evidenced based on ecotoxicology tests, like Phytotoxicity (Satheeshkumar et al., 2024) and geno toxicity studies (Tenorio et al., 2020). Therefore, in the present study, an integrated treatment process for hospital wastewater utilizing the combined effects of electro-oxidation with a hollow cylindrical Ti–TiO_2/IrO_2/RuO_2 mesh electrode and microbial biodegradation by *Priestia flexa* has been developed. The novel mesh electrode is believed to promote higher oxidation generation volume owing its enhanced mass transfer, oxidant generation and high stability all within an optimized current density towards degradation of HWW. In addition, this study represents the first investigation into the biodegradation potential of *P. flexa* with respect to HWW. The results of Ultraviolet-Visible spectroscopy (UV–Vis), Fourier Transform Infrared Spectroscopy (FT-IR), Gas Chromatography Mass Spectroscopy (GC–MS) and Total Organic Carbon (TOC) analyses and few critical environmental parameters are analyzed to support our findings. Therefore, the present investigation would provide an inexpensive, scalable and eco-friendly hybrid electro-biological strategy for sustainable treatment and recycling of HWW.

2. Materials

2.1. Chemicals

High-purity chemicals such as Mineral Salts Medium (MSM) media, Lysogeny broth (LB), ($(CH_3)_2SO_2$), Nutrient Agar (NA), Potassium bromide pellets (KBr), Mercuric sulphate crystals ($HgSO_4$), Potassium Di chromate ($K_2Cr_2O_7$), Ferric Ammonium Sulphate Crystals ($(NH_4)Fe(SO_4)_2.2H_2O$), Silver Sulphate crystals (Ag_2SO_4), Hydrochloric acid (HCL), Nitric acid (HNO_3), Concentrated Sulphuric acid (H_2SO_4), Orthophosphoric acid (H_3PO_4), Potassium Iodide Ammonium Molybdate ($(NH_4)_6Mo_7O_{24}.4H_2O$), Diphenyl amine indicator ($(C_6H_5)_2NH$), Ferroin indicator ($[Fe(C_{12}H_8N_2)_3]SO_4$), Methanol solvent (CH_3OH) and deionised Milli-Q- water were purchased from Hi-Media (Mumbai, India).

3. Methods

3.1. Collection of hospital wastewater

HWW was collected from a hospital in Vellore, Tamil Nadu, India. 25 L of standing water that had been stored for about 20d (days) was collected in a high-density polyethylene Jerrican container. The specimens were taken to Vels University's Microbiology and Molecular Research (MMR) Laboratory, Pallavaram, Chengalpattu, India. The collected sample was kept in a refrigerator at 4–8 °C till subsequent analytical processes.

3.2. Experimental set-up and electro-oxidation process

The EO reactor was made of 8-mm thick glass with a total volume of 600 mL capacity. The chamber (6 × 6 × 11 cm) consisted of a central inlet (0.5 cm) and an extended base (10 × 10 × 4 cm) with a side outlet (0.5 cm). Circulation was maintained by a portable mini water pump. The experimental setup is given in the Supplementary Information (Fig. S1). The electrodes were purchased from Ti Fab Engineering works Chennai, Tamil Nadu. The anode is made of a Titanium (Ti) substrate coated with mixed triple metal oxides (Ti–TiO_2/IrO_2/RuO_2), whereas the cathode is crafted with Ti metal. The anode is designed as a diamond-patterned mesh electrode with a hollow cylindrical structure with dimensions of 3.5 cm in diameter and 8.5 cm in height, In contrast, the cathode is 4.5 cm in diameter and 8.5 cm in height, resulting in the estimated surface area of hollow cylindrical expanded diamond mesh electrode based on the specified geometric parameters which was mentioned in Supplementary Information (S3) (Weusten et al., 2022). The Mesh/Developed area is used to calculate the current density. To operate the EO process on an anode with an area of 78.7 cm^2: (5.8 mA/cm^2 → 0.46 A, 10.4 mA/cm^2 → 0.82 A, 15.5 mA/cm^2 → 1.22 A).

Before the EO experiments, wastewater was mixed for 30 min to homogenize. To facilitate stable electrochemical reactions, the inter-electrode gap is maintained between 8 and 10 mm. The electrodes are connected to a DC power supply, which is used to apply varying current densities (5.8, 10.4, and 15.5 mA/cm^2), allowing for the examination of COD reduction levels at the end of the EO process. The operating cell voltage ranges from 3.9 to 4.8 V (Santhanam et al., 2019). Raw and treated HWW physicochemical parameters were assessed according to APHA (1998) (Baird et al., 2017). The pH (Wellon meter), conductivity (Eutech CON 450), turbidity, Total Dissolved Solids (TDS) and Total Suspended Solids (TSS) were tested by following standard methods APHA (1998). Chloride and sulfate were measured by Mohr's and gravimetric methods, respectively (Baird et al., 2017). Hardness, Ca^{2+} and Mg^{2+} were measured by titration. Total nitrogen forms (NH_3, NO_3^-, NO_2^-) are determined by conventional colorimetric/titrimetric techniques. BOD was measured after 3d of incubation at 27 °C following a standard protocol (IS 3025, 2003), and active chlorine generated during EO was determined iodometrically. COD was quantified by dichromate digestion. Biodegradation tests of raw and bacterial culture (10d and 20d) were analyzed by spectrophotometry (Spectroquant®, Merck). FTIR spectra (4000–400 cm^{-1}, PerkinElmer) were recorded from KBr pellets of the dried samples. GC–MS (Agilent 6890 N/HP 5973 MSD) analysis was conducted on methanol-extracted and 0.22 μm-filtered samples for the identification of organic compounds and degradation products. Initial and final cultures were analyzed for Total Organic Carbon (TOC). Morphological and elemental analysis of the electrode surfaces were conducted via X-Ray Diffraction (XRD) (Bruker D8-ADVANCE) and High Resolution-Scanning Electron Microscope (HR-SEM) using Energy Dispensive X-Ray (EDX) (Thermo Scientific Apreo S). The energy consumption of the EO process was determined by classic electrochemical equations (Vinoth et al., 2025).

$$\text{Energy consumption kWh m}^{-3} = \frac{1}{Vs}\int_0^t VIdt \quad (1)$$

V represents the applied voltage (V), A denotes the applied current (A), t indicates the treatment duration (h), and Vs is the volume of the solution (L).

3.3. Bacterial isolation, identification and biodegradation process

Hospital effluent (1 mL) was serially diluted and plated on nutrient agar using the pour-plate method and incubated at 37 °C for 24 h. Colonies with different morphologies were selected, purified and a series of biochemical tests were performed to confirm the bacterial characteristics. The genomic DNA was extracted and the 16S rRNA gene was PCR amplified with universal primers, sequenced and taxonomically identified as *Priestia flexa*. The culture was preserved on nutrient agar slants at 4 °C and sub-cultured in LB broth for further analyses. An isolated strain was further cultivated in a medium containing 5% MSM to promote bacterial proliferation. Biodegradation experiments were conducted in 250 mL Erlenmeyer flasks, each containing 150 mL of EO-treated HWW and inoculated with 1 mL of the *P. flexa* culture. The flasks were incubated under aerobic conditions at 37 °C with continuous agitation at 150 rpm for a period of 20d. A control setup was established, consisting of 150 mL of EO-treated HWW with 1 mL of MSM (without the bacterial inoculum) to compare the biodegradation efficacy. Bacterial growth was monitored every other day by UV–Vis spectrophotometer (Guo et al., 2021; Phugare and Jadhav, 2015) Shimadzu UV-1800, 200–800 nm) and samples were collected at initial day, 10th d and 20th d for FTIR, GC–MS and TOC analysis to estimate the degradation rates.

3.4. Phytotoxicity assay

The phytotoxicity of untreated HWW and EO-treated Hospital water was assessed with *C. ternatea* sp. (Clitoria) seeds and *C. sativum* (coriander) seeds purchased from the local Vellore market, Tamil Nadu, India. The seeds were surface sterilized with 1% sodium hypochlorite for 2 min and then washed with distilled water several times and were transferred into plastic pots (10 cm dia) filled with pre-autoclaved garden soil. Four to five seeds were sowed in each pot and the seeds were treated with (i) distilled water (control) (ii) raw HWW (iii) EO- HWW (Rahman et al., 2018). Soil water content was kept around 50% and then irrigation with the test solutions was carried out cyclically. Pots were placed outside in full sunlight at ~30 °C and examined for both seed germination and seedling growth over a 20d period. Replicated mean values of percent germination, shoot length and seedling vigor index were taken from triplicates within a treatment.

3.5. Zebra fish embryo toxicity assay

Effect of untreated and EO-treated hospital wastewater (HWW) was tested for embryo toxicity in *Danio rerio* fish embryos according to Organization for Economic Co-operation and Development (OECD) guidelines with few modifications (Tenorio et al., 2020). Fertilized embryos (≤4 hpf) were treated with test solutions in 300 µL embryo medium, in 48-well plates, at concentrations of 5, 10, 15, 20, and 25 µL and with embryo medium only as control. At least 20 embryos from each group were tested in triplicate assays of the tested concentrations. Embryos were checked at 5.25 and 10 h post fertilization (hpf) to eliminate those with clotted or abnormal eggs, and observed at 24, 48, 72, 96, and 120 hpf, using an Olympus CKX41 inverted microscope. Morphological measurements were made based on coagulation/lethality, delayed hatching, tail malformations (curved, elbowed, shortened), edema (head, yolk, pericardial), hemorrhage, cardiovascular malformations, pectoral fin and craniofacial malformations, pigmentation defects, yolk defects, and no tail detachment (Vieira et al., 2021). The survival ability and the frequency of developmental malformations were assessed. Larvae were euthanized with MS-222 (1 g/L) overdose and snap-frozen in liquid nitrogen at the end of final scoring at 120 hpf.

3.6. Statistical analysis

Each experiment was performed out in triplicate ($n = 3$), & the data was displayed using the mean ± standard deviation (SD). Tukey's post hoc test was used to compare treatment group physicochemical parameters after one-way analysis of variance (ANOVA) (GraphPad Prism software) had been performed. Triplicate values in electro-oxidation (EO) study constituted distinct, independently run experiments conducted under the same experimental conditions. Dunnett's test was then used to compare the groups. Statistical significance was established at $p < 0.05$.

4. Result and discussion

4.1. HWW's physicochemical characteristics

The raw HWW was highly polluted with pH 7.42 ± 0.20, turbidty 13 ± 0.10 Nephelometric Turbidity Unit (NTU), TDS 4567 ± 26.0 mg L^{-1}, TSS 2836 ± 21.0 mg L^{-1}, conductivity 1691 ± 5.0 µS cm, hardness 1400 ± 12.5 mg L^{-1}, alkalinity 680 ± 11.5 mg L^{-1}, calcium 480 ± 3.0 mg L^{-1}, magnesium 160 ± 5.0 mg L^{-1}, chloride 1800 ± 16.0 mg L^{-1}, sulfate 980 ± 13.0 mg L^{-1}, total Kjeldahl nitrogen 140 ± 2.0 mg L^{-1}, nitrate 35 ± 2.5 mg $L^{-1}$and ammonia 3.0 ± 0.3 mg L^{-1}, and COD 3000 ± 18.0 mg $L^{-1}$and BOD 1300 ± 9.0 mg L^{-1} which all are were well above the permissible limits according to World Health Organization (WHO). With EO treatment, the water quality was considerably enhanced with reduced turbidity to 4.5 ± 0.10 NTU, TDS to 760 ± 11.4 mg L^{-1}, TSS to 380 ± 8.2 mg L^{-1}, hardness to 280 ± 4.8 mg L^{-1}, alkalinity to 118 ± 6.4 mg L^{-1}, chloride to 860 ± 15.4 mg L^{-1}, and sulfate to 520 ± 9.8 mg L^{-1}, and significant reduction of nitrogenous pollutants and thus attaining 93.16% reduction (3000 ± 18.0 → 205 ± 8.9 mg L^{-1}) in COD and 87.6% in BOD (1300 ± 9.0 → 160 ± 4.5 mg L^{-1}) as well. (Table. 1) displays biological degradation process (BDP) results of reduced turbidity to 3.0 ± 0.10 NTU, TDS to 500 ± 10.0 mg L^{-1}, TSS to 280 ± 7.0 mg L^{-1}, hardness to 200 ± 3.0 mg L^{-1}, alkalinity to 81 ± 5.5 mg L^{-1}, chloride to 57 ± 4 mg L^{-1}, and sulphate to 250 ± 13.0 mg L^{-1}, with complete removal of Total Kjedhal Nitrogen (TKN), nitrate as well as ammonia. In addition, 96.6% COD reduction (3000 ± 18.0 → 100 ± 6 mg L^{-1}) and 95.3% BOD reduction (1300 ± 9.0 → 60 ± 5 mg L^{-1}), thereby complying World Health Organization (WHO) standards (Yi et al., 2007). Higher values of raw HWW physicochemical parameters are due to excessive organic load, nutrients enrichment and high salinity posing threats of eutrophication, microbial contamination and ecotoxicity. However, EO process was found to be successful in degrading recalcitrant organics, oxidizing nitrogenous compounds and diminishing COD and BOD, mostly by hydroxyl radicals and indirect oxidants (i.e., hypochlorite) driven by Ti–TiO_2/IrO_2/RuO_2 anode. Although, it was found ineffective in achieving complete elimination of stubborn anions such as chloride and sulfate which were still above the safe levels. In comparison, the Bio Electro Oxidation (BEO) (Fig. S2) integration led to the maximum or complete pollutant degradation, wherein ionic, nutrient and organic contents were less than or equal to Transformation Zone Type 1 (TZ-1) guidelines, indicating an appreciative collaborative role of bio-degradation along with EO treatment (Abilaji et al., 2023; Aravind et al., 2016). These results indicate that significant removal of recalcitrant's can be made through use of biodegradation system, and thus offering a viable and scalable approach towards treating HWW compliance achieving full compliance with discharge standards. (Fan et al., 2022).

4.2. Electro oxidation process

The oxidation rate of COD by EO of HWW is highly dependent on the applied current density within 7 h HWW treatment time. (Fig. 1) shows the COD removal efficiency of 28% achieved at 5.8 mA/cm^2 62% at 10.4 mA/cm^2. Meanwhile a maximum removal of 96% was obtained at

Table 1
Physiochemical parameters of Raw and Treated (EO) and bio-degradation process.

Parameters	RAW	Treated (EO)	BDP	Acceptable limit	Permissible limit	WHO
Appearance	**Sly-Turbid**	**–**	**Clear**	**–**	**–**	**–**
Colour	**Brownish**	**White**	**White**	**Agreeable**	**Agreeable**	**–**
Odour	**Some odour**	**–**	**–**	**–**	**–**	**–**
pH	**7.42 ± 0.20**	**7.0 ± 0.20**	**6.8 ± 0.20**	**6.5–8.5**	**6.5–8.5**	**6.5–8.5**
Turbidity (NTU)	**13 ± 0.10**	**4.5 ± 0.10**	**3.0 ± 0.10**	**1**	**5**	**–**
Total dissolved solids (mg L^{-1})	**4567 ± 26.0**	**760 ± 11.4**	**500 ± 10.0**	**500**	**2000**	**1500**
Total suspended solids (mg L^{-1})	**2836 ± 21.0**	**380 ± 8.2**	**280 ± 7.0**	**–**	**–**	**–**
Conductivity (μS cm)	**1691 ± 5.0**	**1425 ± 9.8**	**1000 ± 8.0**	**–**	**–**	**–**
Total Hardness	**1400 ± 12.5**	**280 ± 4.8**	**200 ± 3.0**	**200**	**600**	**–**
Calcium	**480 ± 3.0**	**72 ± 2.5**	**50 ± 2.5**	**75**	**200**	**–**
Magnesium (mg L^{-1})	**160 ± 5.0**	**38 ± 2.2**	**38 ± 2.2**	**30**	**100**	**–**
Total Alkalinity (mg L^{-1})	**680 ± 11.5**	**118 ± 6.4**	**81 ± 5.5**	**200**	**600**	**–**
Total Phosphate as PO_4 (mg L^{-1})	**0.9 ± 0.0**	**0.5 ± 0.0**	**0.2 ± 0.0**	**–**	**–**	**0.1**
Chloride (mg L^{-1})	**1800 ± 16.0**	**860 ± 15.4**	**57 ± 4**	**250**	**1000**	**250**
Sulphate (mg L^{-1})	**980 ± 13.0**	**520 ± 9.8**	**250 ± 13.0**	**200**	**400**	**200**
Total Kjedhal nitrogen (mg L^{-1})	**140 ± 2.0**	**0.00**	**0.00**	**–**	**–**	**–**
Ammonia (mg L^{-1})	**3.0 ± 0.3**	**1.0 ± 0.0**	**0.5 ± 0.0**	**0.5**	**0.5**	**2**
Nitrate (mg L^{-1})	**35 ± 2.5**	**10 ± 0.1**	**6.5 ± 0.0**	**45**	**45**	**45**
Nitrite (mg L^{-1})	**0.35 ± 0.0**	**0.08 ± 0.0**	**0.02 ± 0.0**	**–**	**–**	**–**
Oil and Grease (mg L^{-1})	**50 ± 4.0**	**0.0**	**0.0**	**–**	**–**	**–**
Chemical oxygen demand (mg L^{-1})	**3000 ± 18.0**	**205 ± 8.9**	**100 ± 6**	**250**	**500**	**500**
Biological oxygen demand(at 27 °C for 3 days) (mg L^{-1})	**1300 ± 9.0**	**160 ± 4.5**	**60 ± 5**	**–**	**–**	**200**

Physicochemical parameters are reported as **mean ± SD (n = 3)**. Statistical comparisons between raw and treated samples were performed using **one-way ANOVA**, and significant differences relative to raw HWW are indicated, ***p < 0.05***.

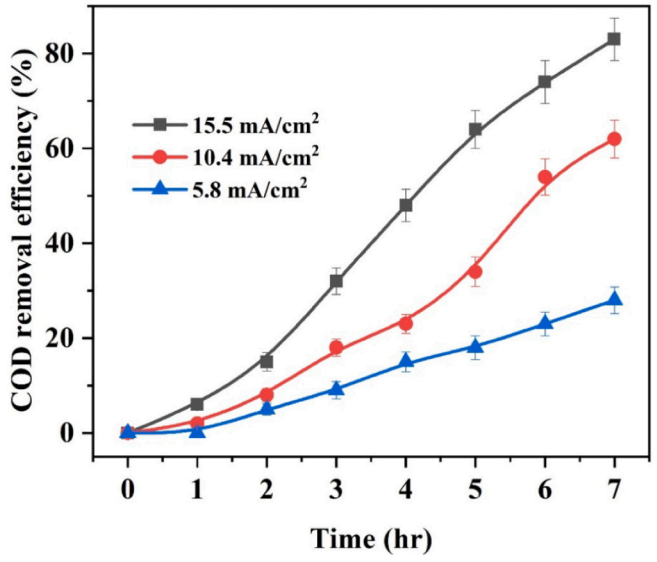

Fig. 1. COD removal efficiency of EO at various current densities.
Data are expressed as mean ± SD of independent EO experiments (n = 3) performed at each current density. Statistical significance among different current densities was evaluated using one-way ANOVA. Differences were considered statistically significant at $p < 0.05$.

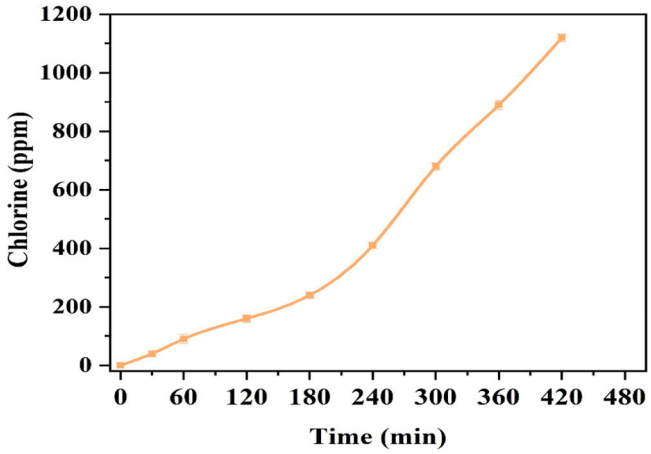

Fig. 2. Electrochemical generation of active chlorine of the EO process at 15.5 mA/cm^2.
Active chlorine concentration values are presented as mean ± SD ($n = 3$) obtained from independent EO runs at 15.5 mA/cm^2. Statistical differences between current densities were analyzed using one-way ANOVA ($p < 0.05$).

15.5 mA/cm^2, which inferred a direct dependence between current and oxidative decomposition of organic matter (Long et al., 2024). The COD removal was calculated as follows:

$$\textbf{Removal efficiency}: N\,(\%) = \left(\frac{\text{Initial value} - \text{Final value}}{\text{Initial value}}\right) * 100 \quad (2)$$

Initial and final pollutant concentrations. Hypochlorite is a strong oxidizer that can oxidize organic matter in wastewater. Simultaneous measurement of active chlorine, free chlorine and hypochlorite concentration at the electrode interface was also found to be proportional to current density, Chlorine concentration increased with increasing current density in the system of 15.5 mA/cm^2, (Fig. 2) which correlated with the highest COD reduction efficiency. The obtained results demonstrated the effectiveness of EO for recalcitrant organics, since higher current intensities promotes the electrochemical generation of reactive oxidizing species, especially free chlorine and hypochlorite, contributing to organics mineralization (Vinoth et al., 2025). Less COD removal efficiency at 5.8 and 10.4 mA/cm^2 may be ascribed to insufficiently generated oxidants that restrict COD oxidation, whereas enhanced COD reduction at 15.5 mA/cm^2 indicates that both direct electron transfer at the anode and indirect oxidation by diffusing chlorine species played a major role at this stage (Dhandapani et al., 2024). The following potential reactions illustrate the possible mechanisms of reducing organic pollutants in the HWW (Hu et al., 2024).

Anodic Reactions:

$$2Cl^- \rightarrow Cl_2 + 2e^- \quad (3)$$

$$6HOCl + 3H_2O \rightarrow 2ClO3^- + 4Cl^- + 12H^+ + 1.5O_2 + 6e- \quad (4)$$

$$2H_2O \rightarrow O_2 + 4H^+ + 6e- \quad (5)$$

Solution reactions:

$$Cl_2 + H_2O \rightarrow HOCl + H^+ + Cl^- \quad (6)$$

$$HOCl \rightarrow H^+ + OCl^- \quad (7)$$

Cathodic reactions:

$$2H_2O + 2e^- \rightarrow 2OH^- + H_2 \quad (8)$$

$$OCl^- + H_2O + 2e^- \rightarrow Cl^- + 2OH^- \quad (9)$$

$$\text{Overall}: 2OH^- + Cl_2 \rightarrow Cl^- + OCl^- + H_2O \quad (10)$$

$$\text{Organic matter} + OCl^- \rightarrow \text{Intermediates organic content} + CO_2 + Cl^- + H_2O \quad (11)$$

The given series of equations proves that the chloride ions are oxidized at the anode ($2Cl^- \rightarrow Cl_2 + 2e^-$) and produce hypochlorite (OCl^-), which will subsequently favors' the oxidation of organic pollutants to CO_2, water and chloride ions, thereby contributing to demineralization (Hu et al., 2024). The enhanced chlorine level at increased current density positively correlated with COD removal efficiency, thus confirming the contribution of active chlorine towards pollutant degradation. The same criteria also seem to favor the inactivation of the bacteria where the oxidative species compromised the integrity of the microbial cells, revealing another promising aspect of EO towards disinfection of healthcare associated effluents (Bhandari et al., 2023). These results indicate that a 15.5 mA/cm^2 is the most effective current density for opening EO and it can be considered as critical criteria of efficient treatment system applicable for treating complicated hospital metal and drug contaminated wastewater.

4.3. Mechanistic perspectives of electro-oxidation kinetics mechanisms

In this work, EO for hospital wastewater was controlled by the interactions of mass transfer, electrode material characteristics and oxidant speciation. The hollow cylinder-shaped Ti–TiO_2 /IrO_2 /RuO_2 mixed metal oxide mesh electrode used in this study had large effective surface area and low diffusion layer thickness, leading to ease of pollutant transport from bulk water to the anode surface and of EO kinetics. Under the optimized current density (15.5 mA cm^2), COD removal reflected on rapid initial degradation governed with reaction-limited kinetics and the later stage of reaction was controlled by mass-transfer limitations. Due to high concentrations of chloride in hospital wastewater, active chlorine species ($HOCl/OCl^-$) mediated indirect oxidation particularly at near-neutral pH where HOCl is predominant. With the surface-produced decomposition of refractory organics begin on the electrode side, where the active chlorine being mainly responsible for bulk oxidation that contributes to an effective mineralization and disinfection. The attained COD removal efficiency (96%) is similar or better than the earlier reported values of such a HWW matrices using CM- Mixed metal oxides (MMO) anodes or boron-doped diamond (BDD) electrodes, operated at a moderate current density (Mosali et al., 2025).

4.4. UV–Vis and FTIR intermediate metabolite identification of Raw and EO treated

The UV–Vis spectra of raw HWW shows broad absorptions at 200–300 nm, due to π–π* transitions from aromatic rings, and at 320–360 nm, due to n–π* transitions from conjugated carbonyl, indicative of the phenolic aromatic pharmaceutical residues and the other chromophoric organic pollutants as seen in (Fig. S3). Upon EO treatment, the intensity of absorbance seems to decrease significantly in these regions, while virtual disappearance is observed at the highest current density value (15.5 mA/cm^2), accounting for decolorization and destruction of chromophoric structures (Ghernaout et al., 2011). Additional evidence of structural alterations in the wastewater is obtained using complementary FTIR analysis. The FTIR spectrum of the raw HWW showed the presence of intense bands at 3450 cm^{-1} (O—H), 2940 and 2855 cm^{-1} (C—H and CH_2 stretching), 1645 cm^{-1} (C═O stretching), 1375 cm^{-1} (CH_3 groups), 1100 cm^{-1} (C—O stretching of alcohols/esters), 995 cm^{-1} (=C–H bending of alkenes) and 620 cm^{-1} (C—Cl stretching), indicating the diverse presence of alcohols, phenols, amides, esters, alkenes and halogenated organics. The peak intensity was significantly reduced in EO-treated sample, where the O—H band appeared at 3425 cm^{-1}, C—H bands at 2930 and 2865 cm^{-1} with lower intensity compared to the C—H bands in the untreated sample. The C═O band shifted to 1640 cm^{-1}, suggests that the aliphatic structures are decomposed partially and carbonyls are oxidized partially. In addition, loss of the = C–H and C—Cl peaks indicated that the unsaturated hydrocarbons and halogenated compounds which are resistant to conventional biological treatment are effectively degraded (Fig. S4). A new peak at 1547 cm^{-1} due to C—N stretching can be assigned to the formation of intermediate amine derivatives upon oxidation, and the C—O peak shifted to 1095 cm^{-1}, with decreased intensity is due to the decomposition of esters and ethers. The presence of a band at 591 cm^{-1} (M–O vibration) suggested that mineral residues are formed from the organic-mineral complexation (Kumari and Tripathi, 2019). Both UV–Vis and FTIR characterizations reveals that the EO has efficiently contributed towards COD reduction by degrading aromatic and conjugated compounds, thus the destruction of molecular structures and mineralizing wide variety of functional groups. This demonstrates the effectiveness of EO process in treating the HWW with high COD removal efficiency at optimum current density.

4.5. HR-SEM and EDAX analysis of the scale deposition on the anode and cathode

SEM-EDX reveals important information about performance and stability of electrode during EO of HWW. After EO process HR-SEM analysis of the electrodes shows the distinctive morphological changes and deposition patterns owing to the longer treatment time of HWW as shown in (Fig. 3). The surface of the anode presented dense and diverse deposits that seemed to agglomerate irregularly in the form of inorganic scales and organic-inorganic composites produced by the oxidation by-products. These findings are further supported by EDX elemental mapping. The cathode spectrum (Fig. 4) primarily composed of oxygen (72.58 wt%, 78.71 wt%) and titanium (16.93 wt%, 6.13 wt%) and had 10.49 wt% (15.16 wt%) carbon and reflected the Ti–TiO_2 matrix with an over layer of oxygen-rich deposits, possibly of carbonate and sulfate precipitates from wastewater. Analysis of the EDX profile of the anode shows high percentage of titanium (49.84 wt%, 67.60 wt%), together with some quantities of ruthenium (47.92 wt%, 30.80 wt%) and smaller amounts of iridium (2.24 wt%, 1.59 wt%) at cathode, (Fig. 4b). The results are in concordance with respect to Ti/TiO_2/IrO_2/RuO_2 mesh anode implying that the catalytic layer is not destructed after EO treatment. The enrichment of oxygen in cathode was attributed to the continuous oxygen production due to high amount of ROS generation and hypochlorite formation, and high concentration of Ru and Ir in anode thus confirming the electrode stability in long-term EO operation. The cathode formation of O-rich phases is in line with the scaling induced by Ca^{2+}, Mg^{2+} and SO_4^{2-} ions present in raw wastewater, forming insulating films that may affect the long-term current efficiency (Zhang et al., 2020). The enrichment of Ti and O implies the retaining of the active material (active TiO_2 layer) to perform oxygen evolution and the generation of reactive chlorine species. On the anode side, the high contents of Ti, Ru, and Ir indicate that the catalytic oxide layer is leachant-resistant thus promotes the electrode lifetime in chloride-rich hospital effluents. The retention of Ru and Ir, which are essential for catalysis, throughout long-term cyclic EO testing, suggests that the electrode design is robust and can provide a constant performance through several EO cycles. These results highlight the fact that, although EO effectively decreases COD and degrades refractory organics.

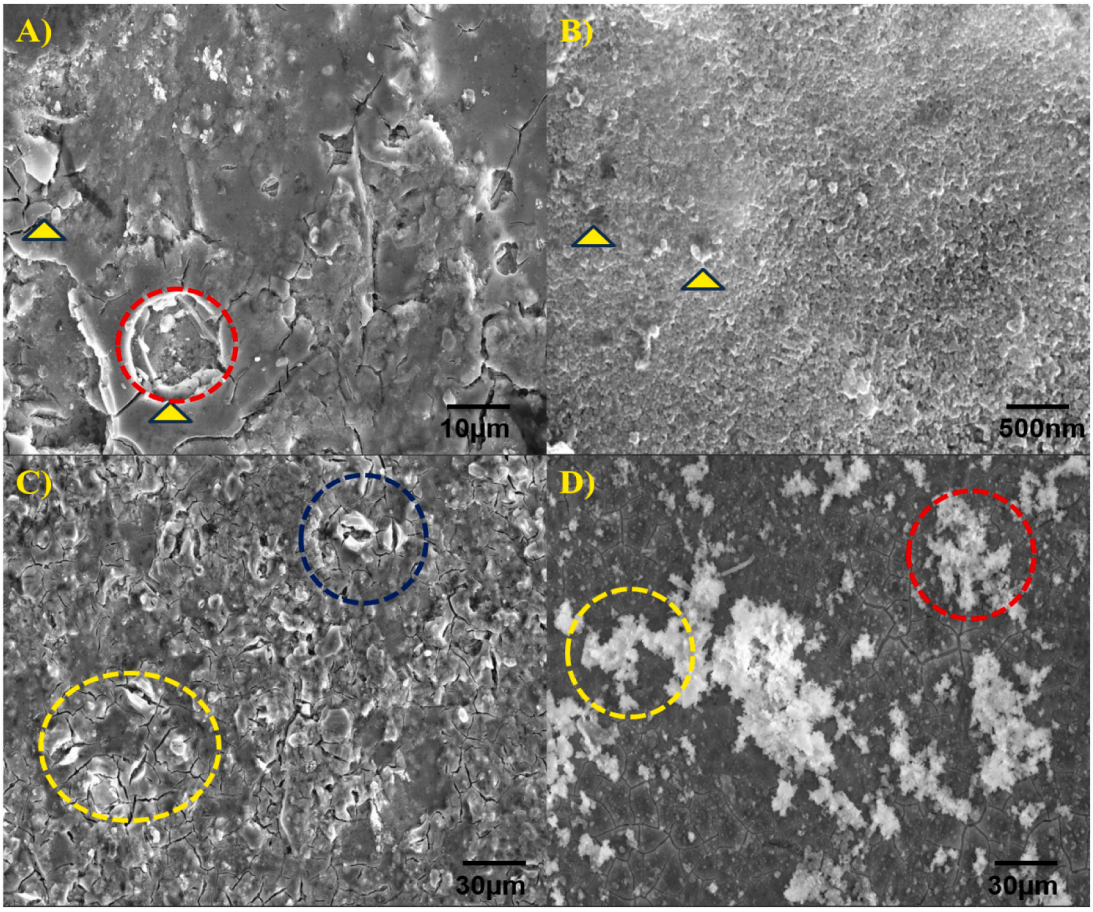

Fig. 3. HR-SEM images of EO electrode after 7 h treatment.

However, scaling of the electrodes is still an issue that requires operational adjustments like changes in current density or pH; intermittent polarity reversal to avoid fouling and maintain the electrode performance. The SEM-EDX analyses not only confirm the mechanistic mechanism of anode-driven oxidation and cathodic deposition, but also illustrate the long-standing utilization of $Ti/TiO_2/IrO_2/RuO_2$ electrodes for HWW, thereby supporting the structural longevity with good pollutant removal efficiency (Sarankumar et al., 2020).

4.6. XRD analysis of EO salt deposition

The XRD diffraction pattern of the deposits obtained during electro oxidation of HWW showed intense crystalline phases corresponding to calcite ($CaCO_3$, JCPDS 01–086-2334), magnesium calcite [$MgCa(CO_3)_2$, JCPDS 01–086-2335] and traces of aragonite, indicating the formation of carbonate minerals at the electrode surface. The strong diffraction peak at ~29.4° 2θ was assigned to the (104) plane of calcite, the main crystalline phase, and the multiple peaks at 23.1°, 36.0°, 39.4°, 43.1°, 47.5°, and 48.5° 2θ could be indexed to representative reflections of magnesium calcite (Fig. S5). The carbonate phases can be attributable to the significant Ca^{2+} and Mg^{2+} concentration found in the raw HWW which has undergone precipitation under electrochemical conditions at high alkalinity near the cathode during EO process (Santhanam et al., 2024). Besides that, carbonate crystallization accounts for the scaling observed in SEM images and provides a reflection of the physicochemical changes occurring in the water in response to EO, in which water electrolysis generates OH^- which increases carbonate super saturation and deposition. Crystalline $CaCO_3$ and $MgCa(CO_3)_2$ phases are found to confirm that EO is able to not only mineralize the organic pollutants but also co-precipitate hardness-causing ions, thus, leading to the enhancement of the quality of water. Overall, the XRD results substantiate the SEM-EDX evidence discussed earlier and provides clear insights into the electrode scaling mechanisms during EO including an assessment of the dual roles of EO in pollutant degradation and coefficient removals of hardness yielding ions from hospital effluents (De Santana Castro et al., 2024).

4.7. Isolation and identification of HWW degrading bacteria

The culture and characterizations of bacterial isolates from hospital wastewater freshly collected resulted in the discovery of a predominant and potential isolate with strong biodegradation capability. Based on 16S rRNA sequencing, (Fig. 5). The molecular studies showed a similarity of 99.7% with *Priestia flexa* (formerly Bacillus) and was submitted to the GenBank National Center for Biotechnology Information (NCBI) (accession no.: PQ220112) for taxonomic estimation (Zhou et al., 2021). Phenotypic and biochemical studies confirmed this identification. The colonies were white, 1–3 mm in diameter, the bacterium was Gram-positive, rod-shaped, spore-forming and motile (Table. S1). The strain showed excellent tolerance for salinity (5–25% NaCl) and grew well within a temperature range of 10 to 40 °C. Biochemical analysis showed (Fig. S6) positive oxidase, catalase, citrate utilization, lysine and ornithine utilization, and negative utilization of indole, methyl red, Voges-Proskauer, and all carbohydrate fermentation tests except urease, representing the versatility of *P. flexa* metabolism (Phan et al., 2023). According to earlier reports, an environmental bacterium isolated from sludge, soil, and wastewater matrices will have an excellent ability to degrade recalcitrant organics, owing to its environmental acclimatization. Based under epi-fluorescent microscopy, bright green fluorescence was apparent in strain *P. flexa* cells after 3d of growth in 2% nutrient

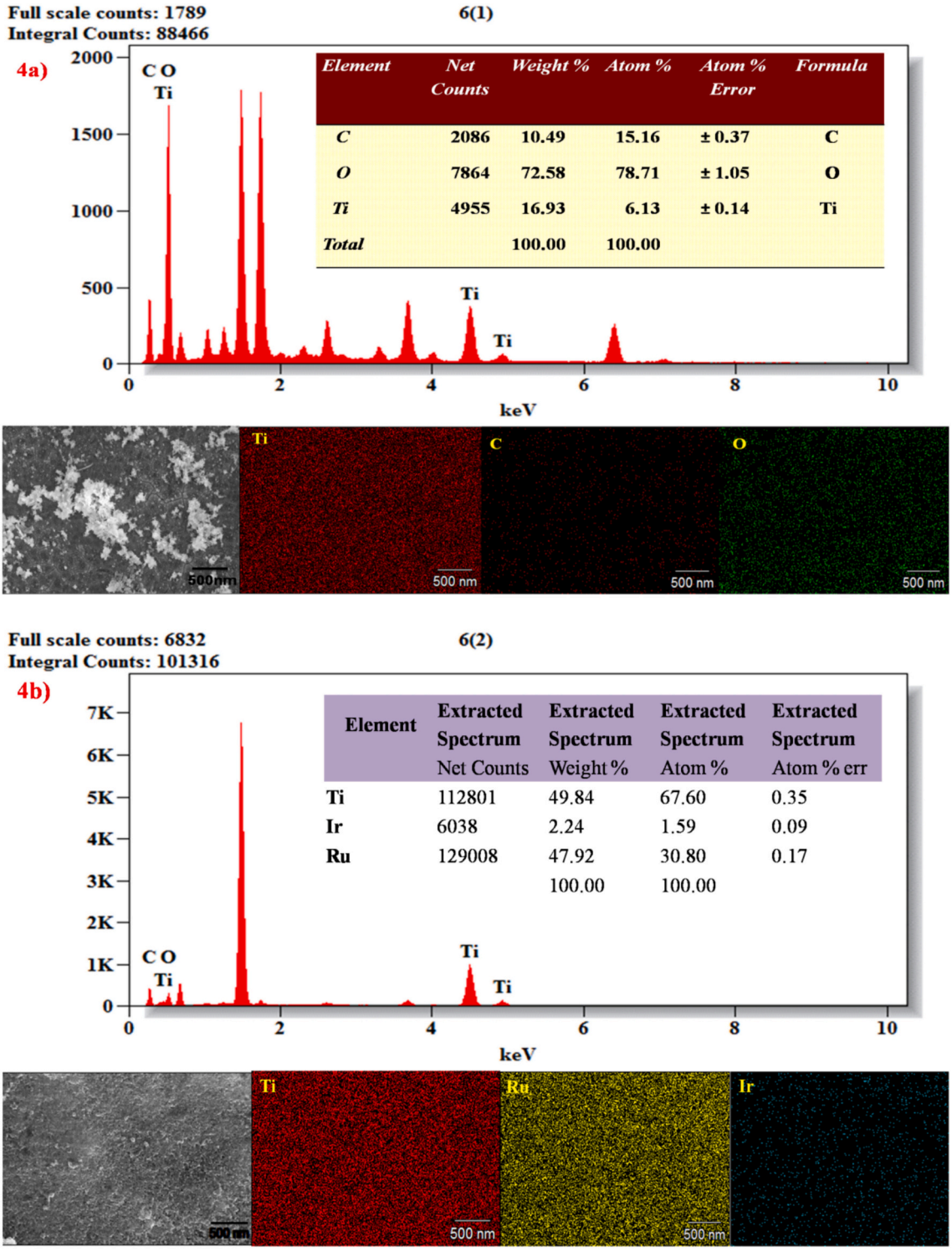

Fig. 4. a: EDAX spectrum of Cathode after 7 h treatment. b: EDAX spectrum of Anode after 7 h treatment.

ROR medium, representing active growth and metabolism in wastewater (Fig. S6). As observed, the decreased UV–vis absorbance over 20d, indicated that even at low concentration, *P. flexa* was effective in degrading toxic organics present in the HWW (Guo et al., 2021). To summarize *P. flexa* features strong physiological properties, superadaptability to extreme wastewater environment, and excellent biodegradation capability, implicating promising characteristics as bioaugmentation bacteria in the treatment of HWW as well as sustainable environmental restoration.

4.8. UV–Vis and FT-IR biodegradation analysis

UV–Vis spectrophotometer analysis was carried out for studying the pollutant degradation occurred during bacterial treatment of HWW. The UV–visible spectrum of the raw sample showed intense absorbance bands around 200–300 nm, and ~ 350 nm (Fig. S7), that are attributed to aromatic compounds, conjugated carbonyls and pharmaceutical residues (Kumar et al., 2025). These peaks intensity decreased especially on day 18d, suggesting the loss of chromophoric organics and

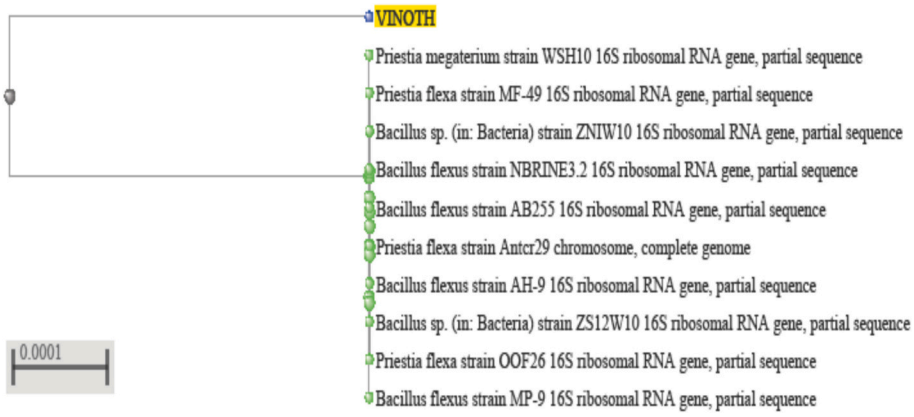

Fig. 5. Phylogenetic tree relationship of bacterial strain *Priestia flexa.*

transformation to simpler, non-absorbing species. The gradual decline in the absorbance as a function of growth indicated active biodegradation by *Priestia flexa*, which mineralized refractory organic pollutants. These findings exhibit the effectiveness of the strain for removal of aromatic and pharmaceutical loads from hospital effluents and can be further implemented for sustainable bioremediation of wastewater (Phugare and Jadhav, 2015). FTIR spectrum analysis revealed that the organic pollutants in HWW were progressively degraded during the 20d of biodegradation process (Fig. 6). Several functional group features associated with complex organic contaminants in the (Initial day) spectrum (Kumar et al., 2025) including broad O—H stretching vibration at 3751 and 3387 cm^{-1}, a C—H stretching vibration at 3383 cm^{-1}, a strong C≡N vibration at 2936 cm^{-1}, and strong C═O stretching bands at 2756, 1752 cm^{-1} are related to aromatic and carbonyl compounds. Other signals at 1653 cm^{-1} (aliphatic CH), 1355 and 1166 cm^{-1} (C—O stretching), 1037 cm^{-1} (=CH), 827 cm^{-1} (M–O vibration), and 619 cm^{-1} (C—Cl stretching) also confirmed the phenolic, esters, amide, halogenated, and metallic-organic complexes characteristic for hospital effluents. By the 10d, extensive spectral changes are observed with decreased intensity of the initial carbonyl and cyanide bands and the presence of some weaker peaks (O—H at 3337 cm^{-1}, aromatic C—H at 2936 cm^{-1}, aliphatic CH at 1643 cm^{-1} and C—O stretching frequencies at 1355 and 1056 cm^{-1}) and the appearance of new aliphatic CH at 947 cm^{-1}.These changes implied the partial oxidation of complex aromatics and generation of intermediate degradation products. The spectra became largely simplified at 20d consisting of residual peaks at 3413 cm^{-1} (O—H), 2925 and 1633 cm^{-1} (C—H stretching), 1344 cm^{-1} (C═C stretching), 1067 cm^{-1} (aliphatic CH), 818 cm^{-1} (O—C stretching), which shows considerably decreased intensity of the band at 560 cm^{-1} (C—Cl stretching) indicating advanced degradation and mineralization

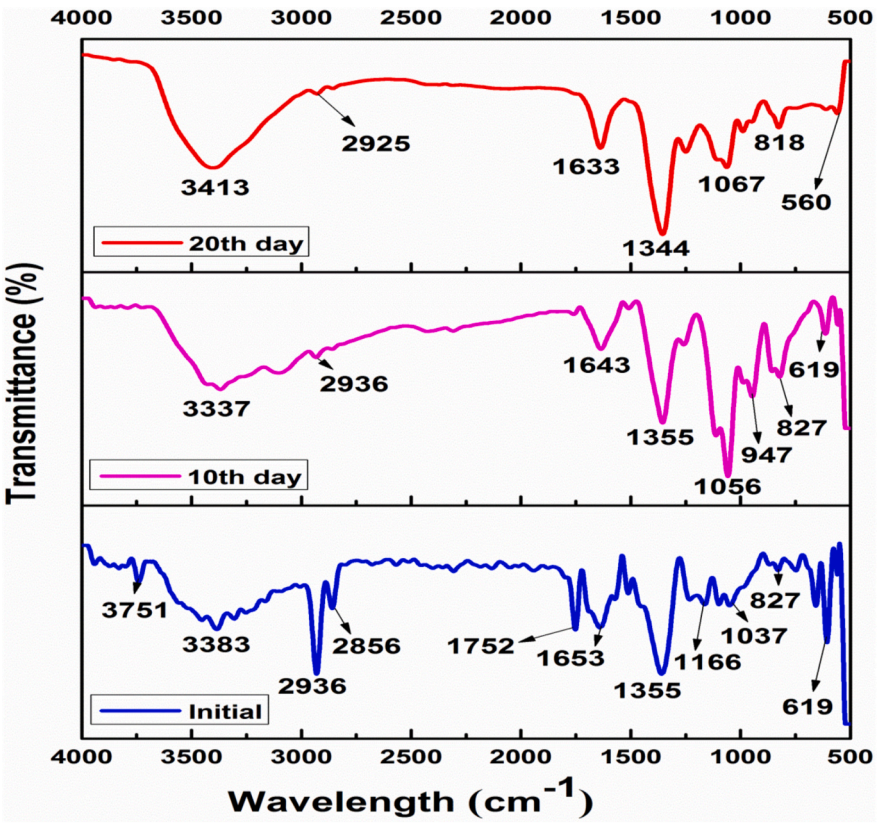

Fig. 6. FT-IR spectra after Biodegradation treatment.

of the majority of the native organic functional groups (Kumari and Tripathi, 2019). The loss/decreased intensity of C≡N, C═O, and = CH bands along with weakened C—Cl stretching suggests that the bacterial strain was capable of oxidative cleavage of the aromatic rings, degradation of halogenated organics and elimination of refractory pharmaceuticals from the mixture. Altogether FTIR emphasized the biodegraded samples in a sequential trend with primary oxidation, intermediate metabolite generation, and near-complete mineralization at 20d indicating the efficiency of the integrated microbial system for HWW and possibility of scalable environmental bioremediation (Kasirajan et al., 2019).

Elevated chloride concentration as well as pharmaceuticals residuals often inhibit bio degradation of HWW due to osmotic and toxic effects on the microbes' metabolism. In the present work, the above said inhibitive effects seem to be diminished by the earlier electro-oxidation step, which simplified the pharmaceutical composition and the ionic strength thus by favouring biodegradation. In addition, the isolated strain *P. flexa* displayed remarkable halo tolerance and metabolic versatility that could steadily live as well as degrade under salty and contaminated environments. The absence of growth inhibition along with COD and TOC decrease during biodegradation suggests that the possible chloride and drug-related inhibitory effects have been successfully relieved by *P. flexa* to treat EO HWW (Dolatabadi et al., 2023).

4.9. Total organic removal efficiency in biodegradation process

The removal of total organic carbon (TOC) yielded quantitative data for the progressive mineralization of organic pollutants present in hospital wastewater in the biodegradation of the slurry. As shown in (Fig. S8) a relatively minor metabolic activity (~20%), associated to the degradation of fast degrading compounds such as simple sugars, amino acids, and short-chain organics, over the 20d incubation period has occurred (Satheeshkumar et al., 2024), By 5-10d the rate of elimination increased to almost 45% suggesting a meditation of active metabolism after the adaptability of the bacterial strain *Priestia flexa*. FTIR analysis showed partial degradation of phenolic and the carbonyl complexes during the Initial-5d period. At 15d, TOC removal is approximately 60% according to the UV–Vis spectrum which showed a pronounced decrease in absorbance of chromophoric organics, indicating further degradation of the resistant pharmaceuticals and the formation of intermediates. The most important difference occurred from day 15–20, where the TOC removal efficiency increased dramatically to 85%, which was an indication of the nearly complete mineralization of organics to CO_2 and H_2O (Mook et al., 2012). This revealed a successful sequential mechanism of EO and biodegradation, wherein initial utilization of simple organics, oxidative removal of complex aromatics, decomposition of intermediates and mineralization. A significant and faster TOC removal at day 20 indicated the potentiality of the strain in effectively minimizing the total carbon load and consequently addressing the environmental footprint of the hospital effluents. These results are in concordance with the metabolic versatility of *P. flexa* established as early as in a wide metabolic profile and support their use as efficient bioremediation agents for sustainable HWW.

4.10. GC–MS biodegradation analysis

The GC–MS analysis of HWW after biodegradation at Initial day, 10d, and 20d showed molecular-level evidence of biodegradation of resistant organics by *Priestia flexa*. GC–MS evidence at molecular level of progressive degradation of recalcitrant organics during biodegradation (Initial day, 10d and 20d) in HWW by Priestia flexa were evident from (Fig. S9a,b,c). The retention times of both parent compounds and degradation products which were found to be highly reproducible (±0.05 min) between sampling intervals. As summarised in (Table. S2a, b, c), higher alkane/hydrocarbon peaks (e.g., docosane and tetradecane, RT 8.34–18.97 min) dominated the initial profile but significantly decreased the 10d and subtended only trace-level peaks by 20d. Aromatic & pharmaceutical related such as naphthalene (RT 13.39 min), quinoline derivates (RT ~ 18.1–18.6), followed a trending conversion accompanied with appearance of often transient oxidized intermediates by 10d. By day-20 GC–MS chromatogram was greatly simplified being comprised mainly with low molecular weight straight-chained aliphatic molecule and organic acids signifying the effective biodegradation/mineralization. The long chain hydrocarbons, aromatic derivatives and pharmaceutical intermediates that consisted of docosane, octadecane derivatives, quinoline compounds, naphthalene, benzene derivatives, fumaric acid esters and cholesterol like molecules are quite evident in the chromatogram (Vaishnavi et al., 2021). The spectrum showed significant changes with those of some parent hydrocarbons disappearing or decreasing while the new peaks of partially oxidized, zed intermediates, such as oleic acid, methyl tridecadienyl ether, histidine derivatives, phthalic acid derivatives and heterocyclic nitrogen compound [quinoline, diazepine, triazole] are appeared (Poddar et al., 2019). This shift suggested a partial cleavage process. The smaller aliphatic compounds, succinic acid derivatives, and alcohols indicate significant mineralization leading to simpler metabolites. The continuous degradation of high molecular weight hydrocarbons and polyaromatics reveals effective biodegradation even at 20d, thus challenging the complex constituents of HWW (Jiao et al., 2023). These GC–MS data are in accordance with TOC, UV–Vis and FTIR measurements and confirmed the efficient decomposition of HWW by *P. flexa* as demonstrated in (Table.2).

4.11. Genotoxicological evaluations

Genotoxicological evaluations of raw and EO treated HWW at 48 hpf & 72 Hours post-fertilization (hpf), was studied with zebra fish embryos HWW. (Fig. 7) displays a time-dependent and concentration-dependent increase in developmental toxicity when treated with 5, 15, and 25 µL. At 48 hpf, the embryos in the 5- µL group presented with an early onset of yolk sac edema and bends on tails while in the 15- µL group the embryos exhibited pericardial and yolk sac edema and decreased pigmentation. By 72 hpf, these defects are exacerbated. The 5 µL group exhibited a lack of proper heart extension, the 15 µL group displayed severe PCE and U-shaped tails, and the 25 µL group presented malformed YSs/continued PCE, revealing cumulative embryo toxicity with the untreated effluent. By contrast, the integrated process treated wastewater exposed embryos at the same concentrations displayed significantly less toxicity (Fig. 7). Both the 5 and 15 µL groups' shows normal development at 48 hpf, with few embryos in the later slightly demonstrating pericardial edema while the 25 µL group shows a mild tail bend, due to somite malformation. By 72 hpf, all the embryos of the treated group at each concentration followed normal development without any morphological deformity (Hoyberghs et al., 2020). (Fig. S10) demonstrates 15 and 25 µL at various dose- and time-dependent shows malformations such as pericardial and yolk sac edema, tail bending, and yolk sac extensions regularly observed in raw HWW, due to the existence of bioactive toxicants, such as heavy metal ions, microbial byproducts, or persistant drug molecules (Fig. S10). Exposure to raw HWW at 72 hpf exhibits cumulative embryo mortality of 20–30% at 25 µL, delayed hatching in >40% of the embryos and sublethal malformations (pericardial edema, yolk sac edema or tail deformities) in more than half of the embryos. On the contrary, embryos exposed to EO-Bio treated wastewater presented >95% survival at all concentrations tested and hatching rates >90%; and malformations were < 5%. The conversion of the more complex contaminants to the less toxic or most inactive form makes the Ti–TiO_2/IrO_2/RuO_2 mesh electrode and biodegradation system, a good decontaminative option to combat embryo toxicity, as evidenced by these results (Vieira et al., 2021). However, the standard chemical indicators such as COD and BOD may not be specifically related to the possible deformations, as observed in embryo responses, which, reveals the necessity of zebra fish bioassays

Table 2
GC–MS retention times demonstrating biodegradation of HWW by *Priestia flexa.*

Retention time (min)	Initial day – major compounds	10d – observed change	20d - residual compounds	Biodegradation inference
8.34 ± 0.05	Docosane, branched alkanes	Peak intensity reduced	Trace docosane	Long-chain alkane degradation
13.39 ± 0.04	Naphthalene	Not detected	Trace naphthalene	Aromatic ring cleavage
14.10 ± 0.03	Tetradecane, pentadecane	Disappeared	Trace tetradecane	Progressive hydrocarbon breakdown
14.97 ± 0.04	Eicosane, octadecane	Disappeared	Minor residual eicosane	Alkane chain shortening
18.11–18.66 ± 0.05	Quinoline derivatives	Oxidized quinoline intermediates	Trace quinoline	Pharmaceutical degradation
27.62–28.74 ± 0.06	Cholesterol, phenanthrene derivatives	Phenanthrenemethanol	Not detected	High-MW aromatic mineralization

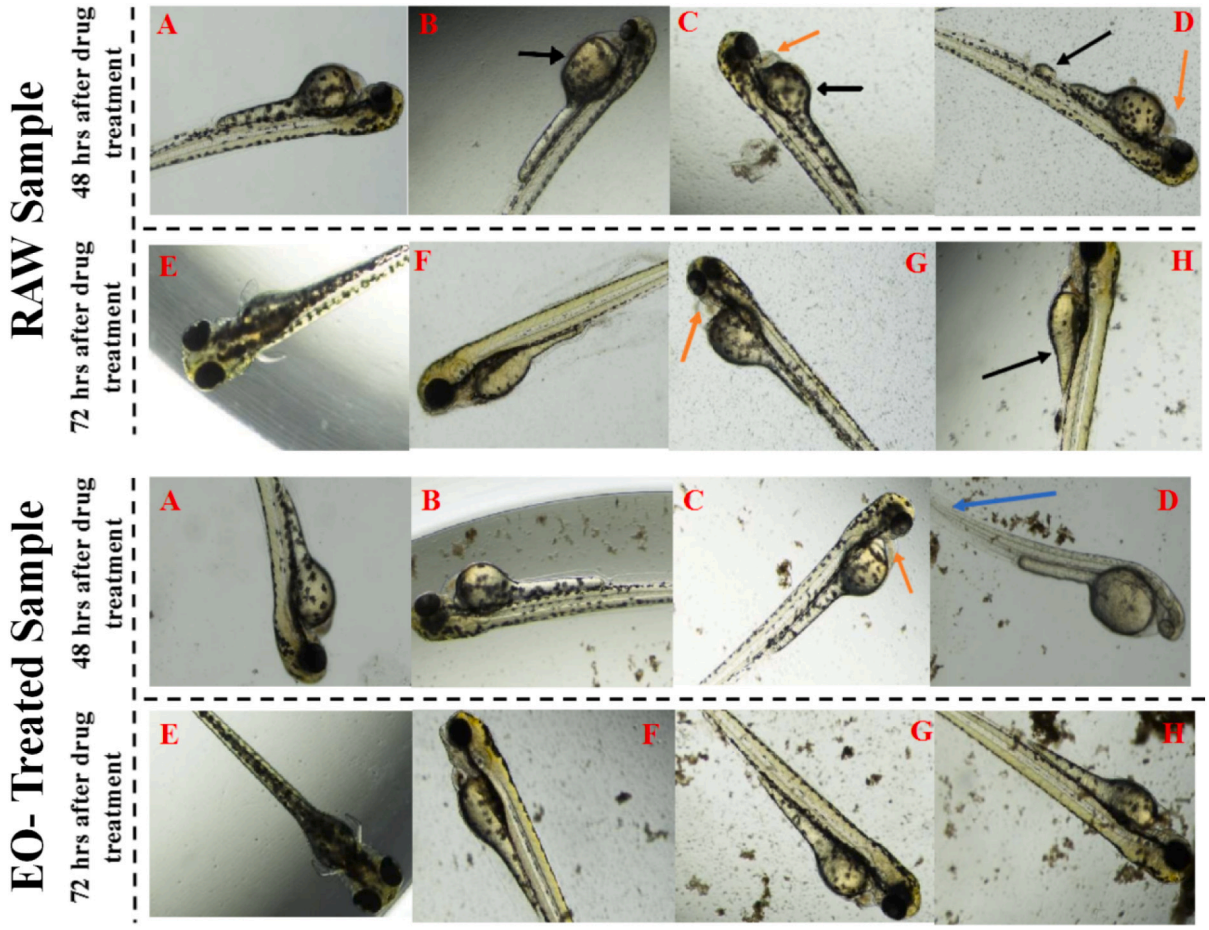

Fig. 7. Genotoxicological assessment of raw and treated hospital wastewater (HWW) using zebrafish embryos at 48 and 72 h post-fertilization (hpf).
RAW Sample: Panels A–D: HWW at 48 hpf showing dose-dependent yolk sac edema, pericardial edema, reduced pigmentation, and tail deformities. **Panels E–H:** Raw HWW at 72 hpf showing aggravated malformations, including severe pericardial/yolk sac edema and axial defects.
EO-treated Sample: **Panels A–D (treated):** HWW at 48 hpf showing largely normal development with only mild, transient abnormalities at higher doses. **Panels E–H (treated):** EO-treated HWW at 72 hpf showing normal morphology across all concentrations. **Orange arrows:** pericardial edema; **Black arrows:** yolk sac edema; **Blue arrows:** tail abnormalities. (For interpretation of the references to colour in this figure legend, the reader is referred to the web version of this article.)

for post-treatment examination.

4.12. Plant toxicity analysis

Seed germination tests with *Clitoria* sp. and *Coriander* sp. were achieved using untreated (control) water (HWW), untreated hospital wastewater (HWW) and EO treated water (Yi et al., 2007). All the test systems showed germination after 5d of incubation and exhibited different growth behavior. In case of *Clitoria,* the seedling was registered at maximum height of 11 cm with treated water followed by 10 cm with control and 8 cm in raw water which confirms the greater growth under EO treated effluent. Similarly, growth of Coriander was maximum (12 cm) in treated water, while it was 9 cm in control and was 6 cm in raw water (Fig. S11). Germination rates and shoot lengths of seeds with untreated HWW are observed to be 60–70% and 6–8 cm respectively. In contrast, treated wastewater absorbed with EO germination was >90% and shoot length 11–12 cm which matched with that of the control treatment. The retarded growth in raw water indicates that untreated HWW has a relative inhibitory impact contributed by its high salinity, organic load and toxic residues. In contrast the non-inhibitory growth using treated water represented a better water quality free of contaminants after EO- Bio integrated treatment (Ahmed et al., 2023). These results indicate that the integrated process of EO- Bio treated hospital effluent not only rendered non-toxic to plants, but may elicited enhancements in growth, which supported its potential use in sustainable irrigation and water management in agriculture.

4.13. Cost analysis

The electrochemical reactor designed for the treatment of the HWW is eco-friendly and economic with comparison with other methods. The reactor can be constructed with standard glass and with acrylic sheets which is cost effective with available materials complemented with mini water pump and silicone tube for an economic design. The cost estimating for the mesh electrode is 1300 and 1850 INR respectively. The materials used here are Titanium for the high efficiency, stability and corrode free in nature as reported in previous studies (Lv et al., 2021). The present study focuses the integrated and sequential biodegradation EO for the removal of organic pollutants in the HWW. Preliminary estimates indicate the treatment cost of 1000 L of hospital wastewater for the EO method, including the electrode cost would be approximately INR 2500. This study provides a cost-effective strategy in incorporating portable reactors in cluster wastewater treatment management. The present attempt would open avenues to develop a pilot scale study in wastewater management and health care facility to discharge treated effluent that can be utilized for agriculture purposes.

4.14. Benefits of the proposed EO–BD approach

The present EO–BD process provides several advantages of conventional and advanced treatment methods for HWW. For the hollow cylindrical Ti–TiO_2/IrO_2/RuO_2 mesh electrode, effective degradation of recalcitrant pharmaceuticals and disinfectants that are difficult to degrade by biological treatment alone can be accomplished using the strong oxidizing power given electrochemically with its three-dimensional mesh nature or realized as a highly active surface area along with more generation of oxidants. Unlike membrane (fouling) and adsorption (secondary solid waste) process, EO is free from fouling, does not generate secondary solid waste and its pretreatment significantly reduces the substrate toxicity and microbial inhibition leading to better bio-degradation efficiency. Unlike ozonation and UV-based advanced oxidation process, the EO process does not need extra chemicals or complex reaction media to produce reactively oxidant with active chlorine species produced on site (in situ) in chloride-rich water. The reactor is small and portable and affordable so that the decentralized treatments can be supported by this EO–BD system in hospitals, which can be an environment-friendly type of treatment (Fan et al., 2022).

4.15. Advantages and limitations

Despite an energy-intensive initial process, EO step and early electrode capital costs associated with the integrated EO–BD system constraints are relatively modest and manageable when applied under an optimum operating condition of this study. The fact that the stable Ti–TiO_2/IrO_2/RuO_2 mesh electrodes can be used for a long time also decreases replacement cycle and lowers cost. Generation of chlorinated by-products in chloride-rich wastewater can be effectively prevented by judicious combination of current density control and subsequent biodegradation, which was supported by the observed decrease in toxicity. In the present study, with the lab-scale tests, a compact mock-up reactor and with appreciable can be up scaled for high volume HWW treatment performance applications. However, any recognised limitations do not seem to have any impact on the functionality of the proposed method but rather indicate potential for future optimisation (Gonzaga et al., 2021).

5. Conclusion

The study demonstrates the combined application of Electro oxidation employing Ti–TiO_2/IrO_2/RuO_2 mesh electrodes and microbial biodegradation mediated by *Priestia flexa* as an effective and sustainable strategy for HWW treatment. Electro oxidation allows rapid pollutant reduction achieving 96% COD removal efficiency at 15.5 mA/ cm^2 in 7 h, which was mediated by the generation of hydroxyl radicals although chloride and sulfate ions residuals. The sequential biodegradation contributed to TOC removal efficiency of 85% via enzyme-mediated mineralization of organic pollutants. The elemental and structural analysis too confirmed the electrode stability. Test trials with EO treated effluent via genotoxicological and phytotoxicity assay determined normal plant growth and elimination of malformations in zebra fish embryos. Overall, the Integrated Electro-Oxidation and Biodegradation approach has proven to be an effective treatment of HWW with contaminant detoxification and assessed ecological safety indication their promise for use in discharge, reuse, and agricultural irrigation.

CRediT authorship contribution statement

Vinoth Kumar Palur Manoharan: Writing – original draft, Methodology, Formal analysis, Data curation, Conceptualization. **Madhan Kumar Pichandi:** Writing – original draft, Validation, Software, Resources, Formal analysis, Data curation. **Adikesavan Selvi:** Writing – review & editing, Validation. **Babujanarthanam Ranganathan:** Validation, Software, Resources, Formal analysis, Data curation. **Sudharsan Kasirajan:** Writing – review & editing, Visualization, Validation, Supervision, Project administration, Methodology, Investigation.

Declaration of competing interest

The authors declare that they have no known competing financial interests or personal relationships that could have appeared to influence the work reported in this paper.

Appendix A. Supplementary data

Supplementary data to this article can be found online at https://doi.org/10.1016/j.biteb.2026.102671.

Data availability

Data will be made available on request.

References

Abilaji, S., Sathishkumar, K., Narenkumar, J., Alsalhi, M.S., Devanesan, S., Parthipan, P., Muthuraj, B., Rajasekar, A., 2023. Sequential photo electro oxidation and biodegradation of textile effluent: elucidation of degradation mechanism and bacterial diversity. Chemosphere 331, 138816. https://doi.org/10.1016/j.chemosphere.2023.138816.

Ahmed, S.N., Ahmad, M., Zafar, M., Aimen, S., Yaseen, G., Rashid, N., Rashid, S., 2023. Morphological and physiological characterization of Coriandrum sativum L. under different concentrations of lead. In: Handbook of Coriander (*Coriandrum sativum*). CRC Press, pp. 85–100. https://doi.org/10.1201/9781003204626.

Akin, B.S., 2016. Contaminant properties of hospital clinical laboratory wastewater: a physiochemical and microbiological assessment. J. Environ. Prot. 7 (5), 635. https://doi.org/10.4236/jep.2016.75057.

APHA, 1998. American public health association. American Water Works Association/Water Environment Federation, Washington DC.

Aravind, P., Subramanyan, V., Ferro, S., Gopalakrishnan, R., 2016. Eco-friendly and facile integrated biological-cum-photo assisted electrooxidation process for degradation of textile wastewater. Water Res. 93, 230–241. https://doi.org/10.1016/j.watres.2016.02.041.

Bagade, O.M., Doke, P.E., 2025. Advancements in combating pathogens in infectious biomedical waste: strategies for pathogen control and health protection. In: Hospital Waste Management and Toxicity Evaluation. IGI Global Scientific Publishing, pp. 191–218. https://doi.org/10.4018/979-8-3693-5757-6.ch007.

Baird, R.B., Eaton, A.D., Rice, E.W., Clesceri, L.S. (Eds.), 2017. Standard Methods for the Examination of Water and Wastewater, 23rd Edition. American Public Health Association (APHA), American Water Works Association (AWWA) and Water Environment Federation (WEF), Washington D.C., USA.

Bhandari, G., Chaudhary, P., Gangola, S., Gupta, S., Gupta, A., Rafatullah, M., 2023. A review on hospital wastewater treatment technologies: current management practices and future prospects. J. Water Process Eng. 56, 104516. https://doi.org/10.1016/j.jwpe.2023.104516.

De Santana Castro, R.S., Doria, A.R., Ferreira, M.B., Eguiluz, K.I.B., Salazar- Banda, G.R., 2024. Advancements in mixed metal oxide anodes for efficient electrochemical

treatment of wastewater. Adv. Chem. Pollut. Environ. Manag. Protect. 10, 191–218. https://doi.org/10.1016/bs.apmp.2023.07.001.
Devda, V., Chaudhary, K., Varjani, S., Pathak, B., Patel, A.K., Singhania, R.R., Chaturvedi, P., 2021. Recovery of resources from industrial wastewater employing electrochemical technologies: status, advancements and perspectives. Bioengineered 12 (1), 4697–4718. https://doi.org/10.1080/21655979.2021.1946631.
Dhandapani, P., Srinivasan, V., Parthipan, P., AlSalhi, M.S., Devanesan, S., Narenkumar, J., Rajamohan, R., Ezhilselvi, V., Rajasekar, A., 2024. Development of an environmentally sustainable technique to minimize the sludge production in the textile effluent sector through an electrokinetic (EK) coupled with electrooxidation (EO) approach. Environ. Geochem. Health 46 (3), 81. https://doi.org/10.1007/s10653-023-01847-7.
Dolatabadi, M., Ehrampoush, M.H., Pournamdari, M., Ebrahimi, A.A., Fallahzadeh, H., Ahmadzadeh, S., 2023. Catalytic electrodes' characterization study serving polluted water treatment: environmental healthcare and ecological risk assessment. J. Environ. Sci. Health B 58 (9), 594–602. https://doi.org/10.1080/03601234.2023.2247943.
Fan, R., Tian, H., Wu, Q., Yi, Y., Yan, X., Liu, B., 2022. Mechanism of bio-electrokinetic remediation of pyrene contaminated soil: effects of an electric field on the degradation pathway and microbial metabolic processes. J. Hazard. Mater. 422, 126959. https://doi.org/10.1016/j.jhazmat.2021.126959.
Ghernaout, D., Naceur, M.W., Aouabed, A., 2011. On the dependence of chlorine by-products generated species formation of the electrode material and applied charge during electrochemical water treatment. Desalination 270, 9–22. https://doi.org/10.1016/j.desal.2011.01.010.
Gonzaga, I.M., Moratalla, A., Eguiluz, K.I., Salazar-Banda, G.R., Cañizares, P., Rodrigo, M.A., Saez, C., 2021. Outstanding performance of the microwave-made MMO-Ti/RuO2IrO2 anode on the removal of antimicrobial activity of Penicillin G by photo electrolysis. Chem. Eng. J. 420, 129999. https://doi.org/10.1016/j.cej.2021.129999.
Guo, D., Guo, Y., Huang, Y., Chen, Y., Dong, X., Chen, H., Li, S., 2021. Preparation and electrochemical treatment application of Ti/Sb-SnO2-Eu&rGO electrode in the degradation of clothianidin wastewater. Chemosphere 265, 129126. https://doi.org/10.1016/j.chemosphere.2020.129126.
Hoyberghs, J., Bars, J.C., Pype, C., Foubert, K., Hernando, M.A., Van Ginneken, C., Ball, J., Van Cruchten, S., 2020. Refinement of the zebrafish embryo developmental toxicity assay. MethodsX 7, 101087. https://doi.org/10.1016/j.mex.2020.101087.
Hu, W., Yang, D., Chang, Y., Yu, K., Yang, L., Yan, W., Xu, H., Wu, X., 2024. Electrocatalytic oxidation for organic wastewater: recent progress in anode material, reactor, and process combination. Chem. Eng. J., 154120 https://doi.org/10.1016/j.cej.2024.154120.
IS 3025, 2003. Part 44 Reaffirmed 2003: Methods of Sampling and Test (Physical and Chemical) for Water and Wastewater, Part 44: Biochemical Oxygen Demand (BOD) by Bureau of Indian Standards.
Jiao, Y., Zhu, Y., Zeng, S., Wang, S., Chen, J., Zhou, X., Ma, G., 2023. Characterization of a novel marine microbial uricase from Priestia flexa and evaluation of the effects of CMCS conjugation on its enzymatic properties. Prep. Biochem. Biotechnol. 53 (7), 816–826. https://doi.org/10.1080/10826068.2022.2145611.
Kasirajan, S., Umapathy, D., Chandrasekar, C., Aafrin, V., Jenitapeter, M., Udhyasooriyan, L., Packirisamy, A.S.B., Muthusamy, S., 2019. Preparation of poly (lactic acid) from Prosopis juliflora and incorporation of chitosan for packaging applications. J. Biosci. Bioeng. 128 (3), 323–331. https://doi.org/10.1016/j.jbiosc.2019.02.013.
Kumar, P.M., Babujanarthanam, R., Selvi, R.T., Ganesamoorthy, R., Sudan, S.J.J., Kasthuri, K., Parameswari, R., 2025. Spherical-shaped ZnO nanoparticles and their diverse surface morphological applications in various biological applications against ROS. Appl. Phys. A Mater. Sci. Process. 131 (5), 379. https://doi.org/10.1007/s00339-025-08504-z.
Kumari, V., Tripathi, A.K., 2019. Characterization of pharmaceuticals industrial effluent using GC–MS and FT-IR analyses and defining its toxicity. Appl Water Sci 9, 1–8. https://doi.org/10.1007/s13201-019-1064-z.
Kumari, A., Maurya, N.S., Tiwari, B., 2020. Hospital wastewater treatment scenario around the globe. In: DBB, pp. 549–570. https://doi.org/10.1016/B978-0-12-819722-6.00015-8.
Long, F., Ghani, D., Huang, R., Zhao, C., 2024. Versatile electrode materials applied in the electrochemical advanced oxidation processes for wastewater treatment: a systematic review. Sep. Purif. Technol., 128725 https://doi.org/10.1016/j.seppur.2024.128725.
Lv, H., Han, P., Li, X., Mu, Z., Zuo, Y., Wang, X., Tan, Y., He, G., Jin, H., Sun, C., Wei, H., Ma, L., 2021. Electrocatalytic degradation of levofloxacin, a typical antibiotic in hospital wastewater. Materials 14 (22), 6814. https://doi.org/10.3390/ma14226814.
Mook, W.T., Chakrabarti, M.H., Aroua, M.K., Khan, G.M.A., Ali, B.S., Islam, M.S., Hassan, M.A., 2012. Removal of total ammonia nitrogen (TAN), nitrate and total organic carbon (TOC) from aquaculture wastewater using electrochemical technology: a review. Desalination 285, 1e13. https://doi.org/10.1016/j.desal.2011.09.029.
Mosali, V.S.S., Soucie, H., Peng, X., Faegh, E., Elam, M., Street, I., Mustain, W.E., 2025. Mechanistic insights into the electrochemical oxidation of acetate at noble metals. Chem Catalysis 5 (2). https://doi.org/10.1016/j.checat.2024.101190.
Nidheesh, P.V., Couras, C., Karim, A.V., Nadais, H., 2022. A review of integrated advanced oxidation processes and biological processes for organic pollutant removal. Chem. Eng. Commun. 209 (3), 390–432. https://doi.org/10.1080/00986445.2020.1864626.
Ogwu, M.C., Ojo, A.O., Alaka, A.C., 2025. Biodiversity and human health: the interconnections of species loss and ecosystem services. In: Innovative Approaches in Environmental Health Management: Processes, Technologies, and Strategies for a Sustainable Future. Springer Nature Switzerland, Cham, pp. 113–141. https://doi.org/10.1007/978-3-031-81966-7_5.
Oliveira, T.S., 2018. Environmental contamination from health-care facilities. J. Health Pollut. 7–19. https://doi.org/10.1016/B978-0-444-63857-1.00002-4.
Oluwole, A.O., Omotola, E.O., Olatunji, O.S., 2020. Pharmaceuticals and personal care products in water and wastewater: a review of treatment processes and use of photocatalyst immobilized on functionalized carbon in AOP degradation. BMC Chem 14 (1), 62. https://doi.org/10.1186/s13065-020-00714-1.
Pariente, M.I., Segura, Y., Alvarez-Torrellas, S., Casas, J.A., De Pedro, Z.M., Diaz, E., Martínez, F., 2022. Critical review of technologies for the on-site treatment of hospital wastewater: from conventional to combined advanced processes. J. Environ. Manag. 320, 115769. https://doi.org/10.1016/j.jenvman.2022.115769.
Phan, H.N.Q., Leu, J.H., Nguyen, V.N.D., 2023. The combination of anaerobic digestion and electro-oxidation for efficient COD removal in beverage wastewater: investigation of electrolytic cells. Sustain 15, 5551. https://doi.org/10.3390/su15065551.
Phugare, S.S., Jadhav, J.P., 2015. Biodegradation of acetamiprid by isolated bacterial strain Rhodococcus sp. BCH2 and toxicological analysis of its metabolites in silkworm (Bombax mori). Clean (Weinh) 43, 296–304. https://doi.org/10.1002/clen.201200563.
Poddar, K., Sarkar, D., Sarkar, A., 2019. Construction of potential bacterial consortia for efficient hydrocarbon degradation. IBB 2019, 144. https://doi.org/10.1016/j.ibiod.2019.104770.
Rahman, M.A., Rayhan, M.Y.H., Chowdhury, M.A.H., Mohiuddin, K.M., Chowdhury, M.A.K., 2018. Phytotoxic effect of synthetic dye effluents on seed germination and early growth of red amaranth. Fundam. Appl. Agric. 3 (2), 480–490. https://doi.org/10.5455/faa.299239.
Santhanam, M., Selvaraj, R., Veerasubbian, V., Sundaram, M., 2019. Bacterial degradation of electrochemically oxidized textile effluent: performance of oxic, anoxic and hybrid oxic-anoxic consortium. Chem. Eng. J. 355, 186–195. https://doi.org/10.1016/j.cej.2018.08.110.
Santhanam, M., Selvaraj, R., Sundaram, M., 2024. A two-step electrochemical method for separating Mg (OH) 2 and CaCO3: application to RO reject and polluted groundwater. Chemosphere 358, 142212. https://doi.org/10.1016/j.chemosphere.2024.142212.
Sarankumar, R.K., Selvi, A., Murugan, K., 2020. Electrokinetic (EK) and bio-electrokinetic (BEK) remediation of hexavalent chromium in contaminated soil using alkalophilic bio-anolyte. Indian Geotech. J. 50, 330–338. https://doi.org/10.1007/s40098-019-00366-6.
Satheeshkumar, A., Duraimurugan, R., Parthipan, P., Sathishkumar, K., AlSalhi, M.S., Devanesan, S., Rajamohan, R., Rajasekar, A., Malik, T., 2024. Integrated electrochemical oxidation and biodegradation for remediation of a neonicotinoid insecticide pollutant. ACS Omega 9 (13), 15239–15250. https://doi.org/10.1021/acsomega.3c09749.
Selvi, A., Rajasekar, A., Theerthagiri, J., Ananthaselvam, A., Sathishkumar, K., Madhavan, J., Rahman, P.K., 2019. Integrated remediation processes toward heavy metal removal/recovery from various environments-a review. Front. Environ. Sci. 7, 66. https://doi.org/10.3389/fenvs.2019.00066.
Tenorio-Chávez, P., Cerro-López, M., Castro-Pastrana, L.I., Ramírez-Rodrigues, M.M., Orozco-Hernández, J.M., Gómez-Oliván, L.M., 2020. Effects of effluent from a hospital in Mexico on the embryonic development of zebrafish, *Danio rerio*. Sci. Total Environ. 727, 138716. https://doi.org/10.1016/j.scitotenv.2020.138716.
Vaishnavi, J., Devanesan, S., Mohamad AlSalhi, S., Rajasekar, A., Selvi, A., Srinivasan, P., Govarthanan, M., 2021. Biosurfactant mediated bioelectrokinetic remediation of diesel contaminated environment. Chemosphere 264, 128377. https://doi.org/10.1016/j.chemosphere.2020.128377.
Vieira, R., Venâncio, C., Félix, L., 2021. Teratogenic, oxidative stress and behavioural outcomes of three fungicides of natural origin (Equisetum arvense, Mimosa tenuiflora, thymol) on zebrafish (Danio rerio). Toxics 9 (1), 8. https://doi.org/10.3390/toxics9010008.
Vinoth kumar, P.M., Dhandapani, P., Madhan kumar, P., Rajasekar, A., Parthipan, P., Vijayaraman, R.S., Prasad, S.M., Kasirajan, S., 2025. Assessment of a hollow cylindrical Ti-TiO2/IrO2/RuO2 mesh electrode for effective treatment of hospital wastewater using a portable electrochemical reactor. J. Indian Chem. Soc., 101985 https://doi.org/10.1016/j.jics.2025.101985.
Weusten, S.J.C., van der Schaaf, J., de Groot, M.T., 2022. Mass transfer in the electrocell microflow and MP cell and the effect of mesh electrodes. J. Electroanal. Chem. 918, 116481. https://doi.org/10.1016/j.jelechem.2022.116481.
Yi, Z., Kangning, C., Wei, W., Wang, J., Lee, S., 2007. Effect of IrO2 loading on RuO2–IrO2–TiO2 anodes: a study of microstructure and working life for the chlorine evolution reaction. Ceram. Int. 33 (6), 1087–1091. https://doi.org/10.1016/j.ceramint.2006.03.025.
Zhang, C., Tang, J., Zhao, G., Tang, Y., Li, J., Li, F., Zhang, Y., 2020. Investigation on electrochemical pilot equipment for water softening with an automatic descaling system: parameter optimization and energy consumption analysis. J. Clean. Prod. 276, 123178. https://doi.org/10.1016/j.jclepro.2020.123178.
Zhou, Y., Cheng, F., He, D., nan Zhang, Y., Qu, J., Yang, X., Chen, J., Willie Peijnenburg, J.G.M., 2021. Effect of UV/chlorine treatment on photo physical and photochemical properties of dissolved organic matter. Water Res. 192. https://doi.org/10.1016/j.watres.2021.116857.